33rd Annual International Conference of the IEEE EMBS
Boston, Massachusetts USA, August 30 - September 3, 2011

Wavelet based data analysis for implantable pulse oximetric sensors

Dominic Ruh, Jens Fiala, Hans Zappe, and Andreas Seifert
Department of Microsystems Engineering (IMTEK), University of Freiburg, Germany,
Email: dominic.ruh@imtek.uni-freiburg.de

Abstract— **Cardiovascular data recording by implantable sensor modules exhibits a number of advantages over extra-corporeal standard approaches. Implantable sensors feature their benefits in particular for high risk patients suffering from chronic heart diseases, because diagnosis can be combined with therapy in a closed loop system. Nevertheless, the measured photoplethysmographic signals reveal different kinds of noise and artifacts. There are several parametric and non-parametric mathematical techniques that try to achieve optimality and generality in estimating the actual signal out of its noisy representation. The determination of blood oxygen saturation and pulse transit time requires one of these mathematical techniques for gaining the exact position and magnitude of maxima and minima in the photoplethysmograph. A robust wavelet algorithm resolves the difficulties arising from physiological data.**

I. INTRODUCTION

We recently presented an implantable sensor concept [1], capable of continuously monitoring vital medical parameters like blood pressure and oxygen saturation. In contrast to state-of-the-art sensor concepts, that are non-portable, our device is an attempt to bridge the gap towards an (24/7) portable sensor system, that facilitates diagnosis and in future stages therapy of various heart defects and chronic diseases, whithout affecting the patients' quality of life. Vital medical parameters need to be measured precisely and as close as possible to their origin to avoid environmental disturbances. MEMS fabrication is the predestinated and preferred technology to bring the sensor as close as possible to the cardiovascular system. Sensor design as well as application area have to be optimized to not interfere with the cardiovascular system. The sensor consists of several optoelectronic devices, that are mounted on a polyimid foil, as shown in Figure 1. During a standard cardiovascular surgery, the sensor is mounted on the vessel wall, without influencing its compliance. Since the transmitted light of several LEDs is detected by a photo-diode, the sensor measures a transmission photophlethysmograph (PPG). Besides pulse shape, this system focuses on the measurement of two vital parameters: Oxygen saturation SpO_2 and pulse-transit time PTT. The latter one correlates with the blood pressure [2]. In order to calculate these two parameters, an exact detection of the extrema close to the systolic slope in the measured PPG is inevitable. SpO_2 is determined by the ordinate of the extrema, while the abscissa of the maxima correlate with the PTT. Different sources of noise as well as motion artifacts affect the sensor signal. Robust signal processing is urgently necessary for preserving the peak positions and peak height in a smooth noise reduced signal representation. In this paper, we present wavelet de-noising as a powerful mathematical technique, to overcome this challenge.

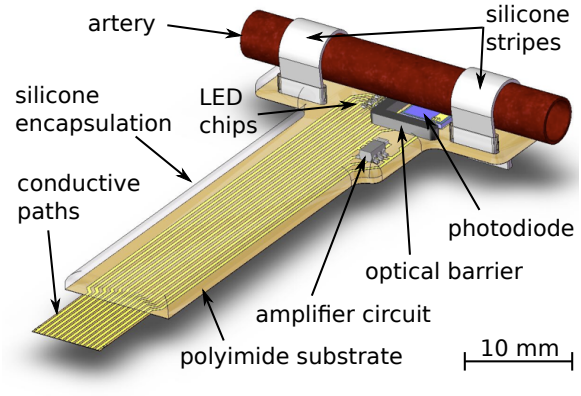

Fig. 1. 3D model of the sensor mounted on an artery.

II. THEORY

Integral transforms are mathematical tools, that simplify the isolation of the real information $s(t)$ from a noisy signal $x(t)$, by mapping the measured noisy signal onto another domain. Since the measured signals are perturbed by irregularities and colored noise, we write

$$x(t) = s(t) + n(t), \tag{1}$$

where the noise $n(t)$ is assumed to be additive. The process of extracting the information $s(t)$ from the signal $x(t)$ is depicted in the following three steps:

1) Transform the signal into an orthogonal domain

$$\tilde{X} = \mathscr{W}(x(t)), \tag{2}$$

2) weight the resulting correlation coefficients in the transform domain by means of a threshold T

$$\tilde{X}_D = \mathscr{D}(\tilde{X}, T) \tag{3}$$

3) and inverse-transform the de-noised signal $\tilde{X}_D$ into its original domain

$$s(t) \approx x_D(t) = \mathscr{W}^{-1}(\tilde{X}_D). \tag{4}$$

In engineering, the most popular orthogonal domain is the frequency domain, where the Fourier transformation is the key to enter and leave. Whereas the Fourier transformation provides a perfect frequency representation of the signal,

while loosing all time information, the wavelet transform allows to depict low frequency details with a low temporal resolution, whereas high frequency details come along with a high temporal resolution. This allows filtering in the time-scale domain. In case of wavelet de-noising, a translation invariant form of the discrete wavelet transform, known as *algoritme à trous* or *stationary wavelet transform*, serves as a tool to enter and leave the wavelet transform domain [3]. Weighting the detail coefficients in the time scale domain for selectively filtering or smoothing the data is called thresholding. In the present case, a non-linear thresholding function applies:

$$\mathscr{D}(\tilde{X},T) = \begin{cases} x-T & \text{if } x \geq T \\ x+T & \text{if } x \leq -T \\ 0 & \text{if } |x| \leq T, \end{cases} \tag{5}$$

where T is the threshold value. The threshold for each decomposition level T_{lev} is given by

$$T_{lev} = \alpha_{lev} \cdot \sigma_{lev} \sqrt{2 \ln N}, \tag{6}$$

where the detail coefficients' standard deviation of each level is estimated by $\sigma_{lev} = \frac{M_{lev}}{0.6745}$. M_{lev} is the median of the detail coefficients, N denotes the number of sample points and α_{lev} is a level dependent factor, according to [4].

III. EXPERIMENTS AND RESULTS

A. In-vivo experiments

The sensor delivers *PPG* measurements in transmission or reflection mode at eight different wavelengths. The present data in this paper were recorded in transmission mode at a wavelength of $\lambda = 650$ nm. Thereby, the sensor was mounted on the carotid artery of a domestic pig during surgery. Figure 2 shows a photo of the applied sensor.

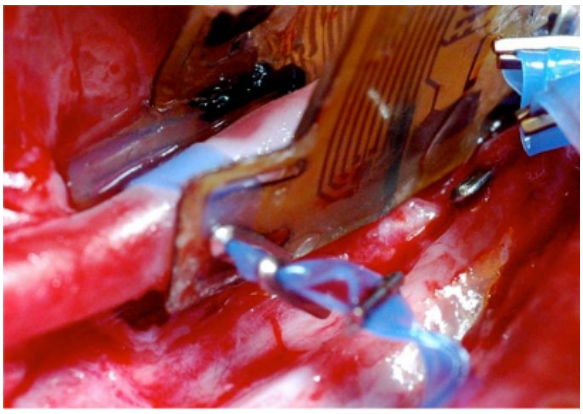

Fig. 2. Transmissive sensor at the carotid of a domestic pig during surgery.

B. Results

In-vivo measurements contain several sources of disturbances, yielding in noisy signals and making it challenging to correctly interpret and analyze the data. Besides electronic noise, like colored noise and spikes, superimposed breathing and motion artifacts negatively influence data analysis.

The sensor signal represents the optical response of the light transmitted through an artery during one cardiac cycle. In a first order approximation, the signal is caused by the vessel wall deformation and hence determined by vessel wall dynamics with complex oscillating excitation. Overtones that arise from this polychromatic excitation of the nonlinear vessel wall mechanics cause this broad frequency spectrum and lead to a small spectral distance of noise and signal. Accordingly, the spectrum of the essential information of the signal roughly lies between 1 and 100 Hz. Additionally, 1/f noise affects this frequency range. The power spectral density *PSD* as well as two pulses of the raw signal from two different experiments are shown in Figure 3 and Figure 4. In 3) the overtones are more pronounced than in 4), while both signals are covered with colored noise. The different frequency characteristics are considered in the de-noising process by the factor α_{lev}, as well as different decomposition levels.

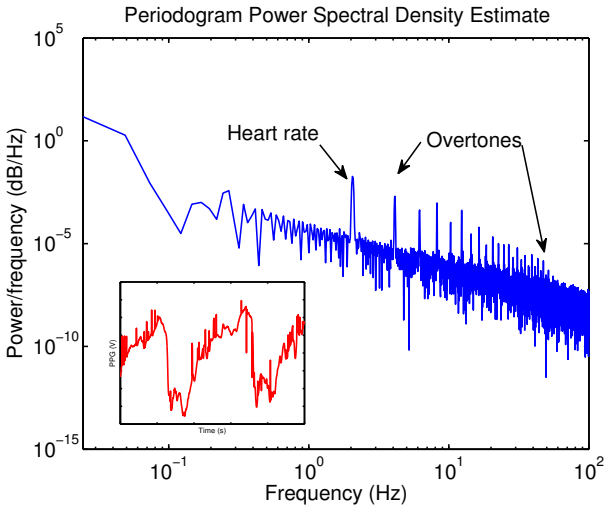

Fig. 3. Power spectral density of a 40s measurement. Lower left corner: Two pulses of the raw-signal in time domain.

The following parameters determine the de-noising procedure introduced in the theory chapter:

- Wavelet
- Decomposition level
- Threshold value
- Thresholding procedure

For both datasets, we used the stationary wavelet transformation algorithm to enter the Daubechies 2 domain. For weighting the correlation coefficients, soft thresholding was employed in both cases. In the first signal, depicted in Figure 5 and referring to the *PSD* of Figure 3, the noise amplitudes are small, but dominant and spikes superimpose the signal. By choosing a decomposition level of $l = 2$ with the parameters α_{lev} to be $\alpha_1 = 1$ and $\alpha_2 = 1/2$, the high frequency components (spikes) of the signal are eliminated, while the high frequency details of the overtones remain unaffected.

In the second case, outlined in Figure 6 and referring to Figure 4, white noise is the dominant factor that reduces

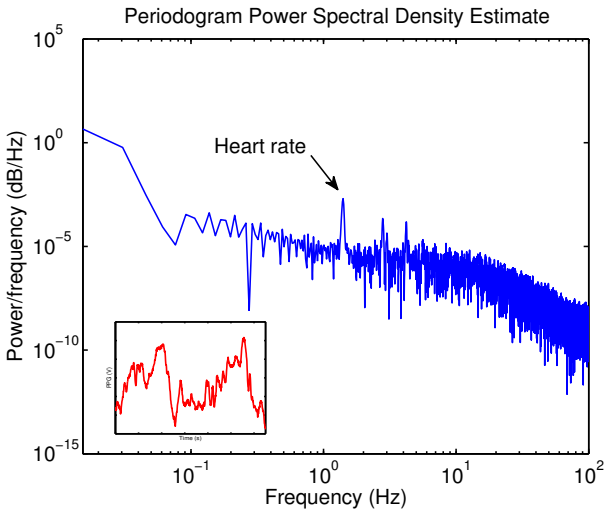

Fig. 4. Power spectral density of a 50s measurement. Lower left corner: Two pulses of the raw-signal in time domain.

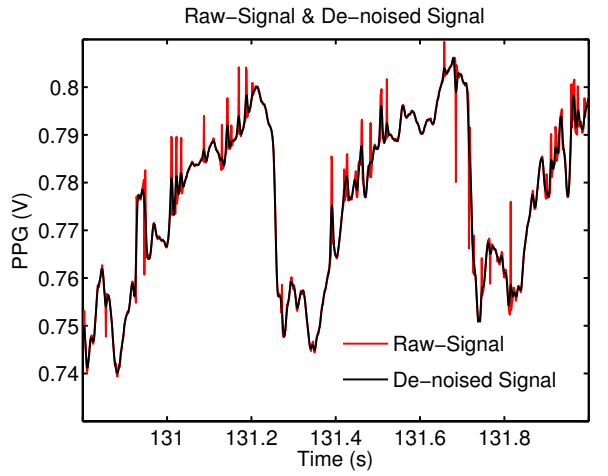

Fig. 5. PPG with random spikes and its de-noised representation.

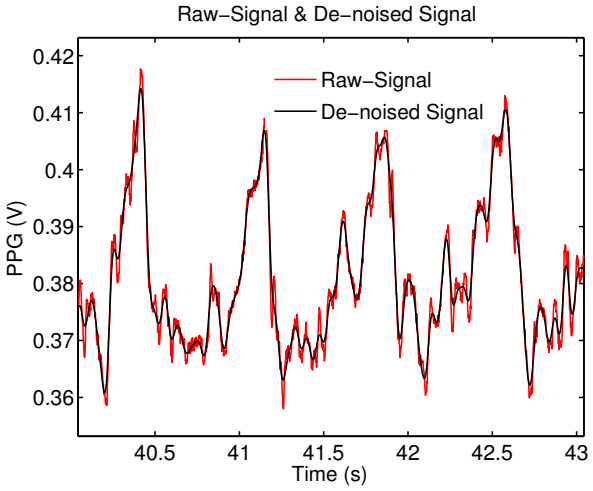

Fig. 6. Noisy signal with smooth approximation due to de-noising.

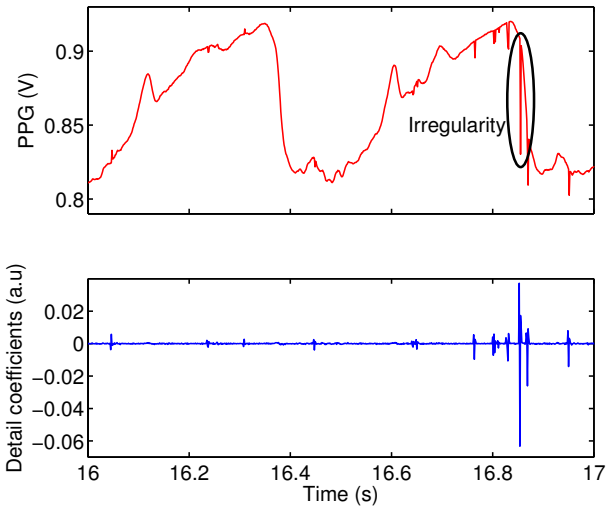

Fig. 7. Two cardiac cycles (*upper plot*) and the associated lowest level detail coefficients (*lower plot*).

the signal-to-noise-ratio. Therefore, the de-noising procedure was performed at a decomposition level of $l = 3$, while the factor α_{lev} equals one for all decomposition levels $\alpha_1 = \alpha_2 = \alpha_3 = 1$. Since the overtones are not as dominant as in the first case, we are able to present the signal in a more smooth way.

An additional feature is given by the *stationary wavelet transform algorithm*. Since the detail coefficients present high frequency details of the original signal, irregularities are easily detected due to thresholding of the detail coefficients as shown in Figure 7. This allows to reveal signal parts which distort the desired actual signal and make it normally impossible to recover the correct information out of such noisy signals. These detected noise components can easily be discarded that way.

IV. CONCLUSIONS AND FUTURE WORKS

A. Conclusions

In this paper we presented wavelet de-noising for *in-vivo* recorded *PPGs*. The parameter α_{lev} was adapted to de-noise two signals, which are superimposed by different kinds of noise. Both results show a good approximation of the *in-vivo* recorded signal, while keeping the signal characteristics. Furthermore, the wavelet decomposition structure simplifies the detection of signal irregularities, due to high detail coefficients.

B. Future Works

At the moment, the parameter α_{lev} is chosen heuristically. Future work will focus on a theoretically well-founded description of the threshold parameters with adaptive thresholding. An operator $d(\cdot)$ has to be designed to determine the adaptive threshold T [5]. The refined method has to be

compared to other signal estimating techniques. Besides this, the sensor's signal-to-noise-ratio will be refined.

V. Acknowledgment

The authors gratefully acknowledge K. Förster, C. Heilmann and F. Beyersdorf from the University Medical Center Freiburg for their valuable advice.

References

[1] P. Bingger, J. Fiala, A. Seifert, N. Weber, K. Foerster, C. Heilmann, F. Beyersdorf, P. Woias, and H. Zappe, "In vivo monitoring of blood oxygenation using an implantable MEMS-based sensor," in *Micro Electro Mechanical Systems (MEMS), 2010 IEEE 23rd International Conference on*. IEEE, 2010, pp. 1031–1034. [Online]. Available: http://ieeexplore.ieee.org/xpls/abs_all.jsp?arnumber=5442385

[2] J. Fiala, P. Bingger, K. Foerster, C. Heilmann, F. Beyersdorf, H. Zappe, and A. Seifert, "Implantable Sensor for Blood Pressure Determination via Pulse Transit Time," in *Sensors, 2010 IEEE 9th Annual IEEE Conference on*, 2010, pp. 1226–1229.

[3] R. Coifman and D. Donoho, "Translation-invariant de-noising," *LECTURE NOTES IN STATISTICS-NEW YORK-SPRINGER VERLAG-*, pp. 125–125, 1995. [Online]. Available: http://stat.stanford.edu/˜donoho/Reports/1995/TIDeNoise.pdf

[4] D. Donoho, "De-noising by soft-thresholding," *IEEE Transactions on Information Theory*, vol. 41, no. 3, pp. 613–627, May 1995. [Online]. Available: http://ieeexplore.ieee.org/lpdocs/epic03/wrapper.htm?arnumber=382009

[5] C. Taswell, "The what, how, and why of wavelet shrinkage denoising," *Computing in science & engineering*, vol. 2, no. 3, pp. 12–19, 2000. [Online]. Available: http://ieeexplore.ieee.org/xpls/abs_all.jsp?arnumber=841791